



HAL
open science

Farnesoid X receptor alpha ligands inhibit HDV in vitro replication and virion infectivity

Anne-Flore Legrand, Julie Lucifora, Benoît Lacombe, Camille Ménard, Maud Michelet, Adrien Foca, Pauline Abrial, Anna Salvetti, Michel Rivoire, Vincent Lotteau, et al.

► To cite this version:

Anne-Flore Legrand, Julie Lucifora, Benoît Lacombe, Camille Ménard, Maud Michelet, et al.. Farnesoid X receptor alpha ligands inhibit HDV in vitro replication and virion infectivity. *Hepatology Communications*, 2023, 7 (5), pp.e0078. 10.1097/HC9.0000000000000078 . hal-04072355

HAL Id: hal-04072355

<https://hal.science/hal-04072355>

Submitted on 18 Apr 2023

HAL is a multi-disciplinary open access archive for the deposit and dissemination of scientific research documents, whether they are published or not. The documents may come from teaching and research institutions in France or abroad, or from public or private research centers.

L'archive ouverte pluridisciplinaire **HAL**, est destinée au dépôt et à la diffusion de documents scientifiques de niveau recherche, publiés ou non, émanant des établissements d'enseignement et de recherche français ou étrangers, des laboratoires publics ou privés.

Farnesoid X receptor alpha ligands inhibit hepatitis delta virus *in vitro* replication and virion infectivity

Anne-Flore Legrand^{1,2,*}, Julie Lucifora^{2,3,*}, Benoît Lacombe¹, Camille Ménard¹, Maud Michelet⁴, Adrien Foca¹, Pauline Abrial¹, Anna Salvetti², Michel Rivoire⁵, Vincent Lotteau¹, David Durantel^{2,3,\$}, Patrice André^{1,2,\$}, and Christophe Ramière^{1,2,6}

Affiliations

¹CIRI, Centre International de Recherche en Infectiologie, Team VIRIMI, Univ Lyon, Inserm, U1111, Université Claude Bernard Lyon 1, CNRS, UMR5308, ENS de Lyon, F-69007, Lyon, France

² University of Lyon, Université Claude Bernard Lyon, Villeurbanne, France.

³ CIRI, Centre International de Recherche en Infectiologie, Team HepVir, Univ Lyon, Inserm, U1111, Université Claude Bernard Lyon 1, CNRS, UMR5308, ENS de Lyon, F-69007, Lyon, France

⁴INSERM, U1052, Cancer Research Center of Lyon (CRCL), University of Lyon (UCBL1), CNRS UMR_5286, Centre Léon Bérard, Lyon, France

⁵INSERM U1032, Centre Léon Bérard (CLB), Lyon, France

⁶Virology Laboratory, Hospices Civils de Lyon, Hôpital de la Croix-Rousse, Lyon, France

*These authors contributed equally to this work

\$These authors contributed equally to this work

Keywords

HDV; FXR; bile acids; hepatocytes; antiviral activity

Contact information

Dr Christophe Ramière

International Center for Infectiology Research (CIRI), Team: Cellular biology of viral infections, INSERM U1111, 21 avenue Tony Garnier, 69007 Lyon, France; Phone: +33 4 37 28 24 47; Fax: +33 4 37 28 23 41; E-mail: christophe.ramiere@inserm.fr

List of Abbreviations

HDV: hepatitis D virus; HBV: hepatitis B virus; BA: bile acids; FXR: farnesoid X receptor alpha; PHH: primary human hepatocyte; HBsAg: Hepatitis B virus surface antigen; peg-IFN- α : pegylated interferon alpha; SVR: sustained virological response; HDAg-S: small hepatitis delta antigen; HDAg-L: large hepatitis delta antigen; NTCP: Na⁺-taurocholate cotransporting polypeptide; dHepaRG: differentiated HepaRG cells; NR: nuclear receptor; CYP7A1: cytochrome P450 family 7 subfamily A member 1; BSEP: bile salt export pump; SoC: standard of care; HNF4A: hepatocyte nuclear factor-4; TR: tetracycline repressor; vge: viral genome equivalent;

Financial support

This work was supported by the grant N° ECTZ136480 from ANRS (French national agency for research on AIDS and viral hepatitis), INSERM annual recurrent fundings, and an Enyo Pharma/INSERM collaboration contract (to VIRIMI team).

Conflict of interest statement

None

Author contributions

- study concept and design: CR, JL, PAn, DD
- acquisition and analyses of data: AFL, JL, BL, MM, AS, CM, AF, PAb, CR
- interpretation of data: CR, AFL, JL, BL, DD, PAn, VL
- drafting of the manuscript: CR, AFL, JL, DD, BL, VL
- funding acquisition: CR, JL, DD, VL, PAn
- material support: MR

Acknowledgments

The authors want to thank Ms Laura Dimier, Jennifer Molle, Océane Floriot and Anaëlle Dubois for their great help with the isolation of primary human hepatocytes, as well as the staff from Prof Michel Rivoire's surgery room for providing us with liver resection.

The authors also want to thank Janssen for the kind gift of anti-HDAg antibodies.

Abstract

Background and Aims: Hepatitis delta virus (HDV), a satellite of hepatitis B virus (HBV), is responsible for the most severe form of human viral hepatitis, for which curative therapy is still awaited. Both HBV and HDV use the hepatic transporter of bile acids (BA) (*i.e.* NTCP) to enter hepatocytes. We previously showed that ligands of the farnesoid-X-receptor alpha (FXR), a master regulator of BA metabolism, inhibit HBV replication. Here we asked whether FXR ligands can also control HDV infection.

Approach & Results: *In vitro* HDV mono-infections or HDV/HBV co-infections and super-infections were performed in differentiated HepaRG cells (dHepaRG) and primary human hepatocytes (PHH). Following treatment with FXR ligands, HDV RNAs and antigens were analyzed by RT-qPCR, northern blot, immunofluorescence and western

blot. Virus secretion was studied by RNA quantification in supernatants and infectivity of secreted HDV particles was measured by re-infection of naive HuH7.5-NTCP cells.

In HDV/HBV superinfection models, a 10-day treatment with FXR ligand GW4064 decreased intracellular HDV RNAs by 60% and 40% in dHepaRG cells and PHH, respectively. Both HDV genomic and antigenomic RNAs were affected by treatment, which also reduced the amount of intracellular delta antigen. This antiviral effect was also observed in HDV monoinfected dHepaRG cells, abolished by FXR loss of function, and reproduced with other FXR ligands. In HBV/HDV coinfecting dHepaRG cells, HDV secretion was decreased by 60% and virion specific infectivity by >95%.

Conclusions: FXR ligands both inhibit directly (*i.e.* independently of anti-HBV activity) and indirectly (*i.e.* dependently of anti-HBV activity) the replication, secretion and infectivity of HDV. The overall anti-HDV activity was superior to that obtained with interferon- α , highlighting the therapeutic potential of FXR ligands in HDV-infected patients.

Introduction

Hepatitis delta virus (HDV) is a defective and satellite virus of hepatitis B virus (HBV), requiring HBV surface antigens (HBsAg) for its propagation. HDV coinfection or superinfection in HBV carriers are characterized by a more rapid progression to liver fibrosis and an increased risk of end-stage and lethal liver diseases (1,2). The exact prevalence of HDV infection is unknown. According to recent meta-analyses, it is estimated that HDV infects between 12 and 60 million people worldwide, which

corresponds to 4.5-13 % of HBV-infected patients, with significant geographic variations of prevalence (1,3,4).

Current therapies relying mainly on pegylated interferon-alpha (Peg-IFN α) are unsatisfactory, as a sustained virological response (SVR) following cessation of treatment is only obtained in a very limited number of patients (5,6). Recently, the HDV entry inhibitor Bulevirtide (also widely known as Myrcludex) was approved in the European Union for the treatment of HDV patients with compensated liver disease, but optimal treatment duration and SVR remain to be determined (7). A few investigational antiviral approaches are currently being tested, but it is widely admitted that novel specific antiviral strategies will be necessary to foster an HDV cure.

Replication of the HDV genome, a 1.7 kb single-stranded negative-sense circular RNA, takes place in the nucleus of infected hepatocytes. Antigenomic RNAs are synthesized by a rolling circle mechanism and serve as templates for the synthesis of new genomic RNAs. Viral mRNAs are also synthesized and encode the small and large delta antigens (HDAg-S and HDAg-L) from a unique open reading frame (8). Compared with HDAg-S (195 amino-acid long), HDAg-L contains an additional domain of 19–20 AA at its C-terminus, which results from an Adenosine Deaminase RNA Specific 1 (ADAR-1)-mediated RNA editing of the antigenomic HDV RNA at a location corresponding to the stop codon of HDAg-S gene (9). This additional domain contains a CXXX-box motif, allowing the addition of a farnesyl group to the cysteine by a cellular farnesyltransferase activity. While HDAg-S is essential to HDV replication, farnesylated HDAg-L inhibits the replication step but favors virus egress (10,11). HDV assembly is initiated by the interaction between HDAg-L and newly synthesized genomic RNAs. These neo-formed ribonucleoproteins, which also contain HDAg-S moieties (12), are then exported from the nucleus to bud into HBsAg empty subviral particles (*i.e.* devoid of HBV

nucleocapsids), supposedly at the endoplasmic reticulum, to generate HDV infectious particles (13). Aside from the crucial role of HBV envelope proteins in the production of infectious HDV particles, the other steps of the HDV life cycle are not dependent on HBV. Bearing HBV envelope proteins at their surface, HDV infectious virions use the same entry receptor as HBV to enter hepatocytes, *i.e.* the sodium taurocholate cotransporting polypeptide (NTCP) (14). NTCP is the main transporter of bile acids (BA) at the basolateral membrane of hepatocytes and several studies suggested that HBsAg-containing particles and BAs compete for binding to NTCP. Indeed, it has been shown that high concentrations of taurocholate inhibit both HBV and HDV entry into differentiated HepaRG cells (dHepaRG). Inversely, binding of the HBsAg preS1 domain to NTCP blocks NTCP-mediated BA uptake in HepG2-NTCP cells (15,16). Even though HDV uses NTCP to enter hepatocytes, the link between BA metabolism and HDV life cycle remains to be explored. BA metabolism homeostasis is maintained by a complex interplay between the liver and gut, in which the farnesoid-X-receptor alpha (FXR), the liver-enriched nuclear receptor (NR) of BA, plays a key role by directly or indirectly regulating the transcription of numerous genes. FXR activation in response to increased intracellular BA concentrations leads to its down-regulation (via a negative feedback loop), a decreased BA entry into enterocytes and hepatocytes, as well as an increased BA excretion into bile ducts via the regulation of several BA transporters expression (*e.g.* the bile salt export pump BSEP). In addition, synthesis of primary BA from cholesterol is inhibited in the liver, in particular following repression of Cytochrome P450 Family 7 Subfamily A Member 1 (CYP7A1) enzyme expression (17).

In our previous work, we showed that FXR can bind to two FXR response elements on the HBV genome (18). Other studies have shown that HBV infection modified the expression of FXR and its target genes in the humanized mouse model and liver biopsies

from chronically infected patients (19). Importantly, we and others have shown that some FXR agonists inhibit HBV replication *in vitro* (20,21). This led to the clinical evaluation, in monotherapy or combination with standards of care (SoC), of the FXR agonist Vofesoxar, as a potential anti-HBV asset (22).

Here we addressed the question of whether FXR and BA metabolism could also play a role in the HDV life cycle, and whether this could be of therapeutic interest. Using relevant cell culture models (primary human hepatocytes (PHH) and dHepaRG cells), we showed that treatment with FXR ligands leads to a moderate inhibition of HDV intracellular replication, irrespective of HBV presence, but a strong decrease of HDV virion secretion, and a very potent reduction of their specific infectivity. These data open perspectives for the treatment of hepatitis delta with FXR ligands.

Materials and Methods

Plasmids and viruses

HDV-1 replication-competent plasmid (pSVLD3) and HBV envelope protein (genotype D) encoding pT7HB2.7 plasmid were kind gifts from Camille Sureau (INTS, France). HDV viral stocks were obtained by transfection of HuH7 cells with plasmids pSVLD3 and pT7HB2.7, as previously described (23). HBV viral stocks were produced from HepAD38 cells, as described before (24).

Chemicals

FXR agonist GW4064 was purchased from Sigma-Aldrich (St. Quentin Fallavier, France), 6 α -Ethyl-Chenodeoxycholic Acid (6-ECDCA) from MedChemExpress (Monmouth Junction, NJ, USA) and tropifexor from ProbeChem (Shanghai, P.R. China).

Interferon-alpha2a was purchased from PBL Assay Science (Piscataway, NJ, USA), and lamivudine from Selleckchem (Houston, TX, USA).

Cell culture and infections

HepaRG cells were cultured, differentiated, and infected by HBV and HDV as previously described (25,26).

PHH were freshly prepared from human liver resection obtained from the Centre Léon Bérard (Lyon) with French ministerial authorizations (AC 2013-1871, DC 2013 – 1870, AFNOR NF 96 900 Sept 2011) as previously described (27).

A polyclonal HepaRG-TR-Cas9 cell line was generated by dual lentiviral transduction (T-Rex system from Invitrogen/ThermoFischer) leading to the stable chromosomal integration of two transgenic expression cassettes, one constitutively coding the tetracycline repressor protein (TR) and another coding upon tetracycline induction (two binding sequences for TR in the promoter/+1 transcription region) the *Streptococcus pyogenes* Cas9 protein.

HuH7.5 cells were kindly provided by C.M. Rice (Rockefeller University, USA). Derived HuH7.5-NTCP cells were generated by lentiviral transduction (28).

Analysis of specific infectivity and density of secreted HDV particles

Supernatants from dHepaRG infected with both HBV and HDV were concentrated using 8 % PEG 8000. HDV RNA was quantified by RT-qPCR in concentrates and HuH7.5-NTCP cells were infected using the same viral genome equivalents (vge) for each condition of

treatment. At indicated times, total cellular RNA was extracted and HDV RNA was quantified by RT-qPCR.

In parallel, concentrated viruses were characterized by analysis of fractions from 20-44% iodixanol gradients. Twelve fractions of 1mL were collected and used for quantification of HDV RNA and HBV DNA by qPCR, HBsAg dosage by ELISA and HDAg and HBsAg detection by western blot.

Methods for nucleic acid quantification, siRNA transfection, HBs and HBe quantification by ELISA and western blot and immunofluorescence analyses are described in the supplementary methods section.

Results

FXR ligand GW4064 decreases intracellular levels of HDV RNAs and proteins in both HBV-infected dHepaRG cells and PHH superinfected with HDV.

The anti-HDV activity of the synthetic FXR ligand GW4064 was first evaluated in dHepaRG cells infected with HBV and superinfected with HDV; such a protocol was initially used as it best mimics *in vivo* infections. IFN- α , which can be considered as the current SoC for HDV in its pegylated form, was used as a control. In superinfected dHepaRG cells, a 10-day treatment with GW4064 decreased the amount of total intracellular HDV RNAs in a dose-dependent manner, reaching 66 % of inhibition at 10 μ M of GW4064 (**Fig. 1A**). Of note, the same levels of inhibition were obtained with a supraphysiological dose of IFN- α (1000 IU/mL), thus suggesting a superiority of the FXR agonization over type-I IFN receptor engagement.

Then, we analyzed intracellular HDV antigens, *i.e.* HDAg-S and HDAg-L by western blot and immunofluorescent staining. Treatment with GW4064 decreased intracellular amounts of both HDAg-S and HDAg-L in the same proportions, by 50% at 1 and 5 μ M of GW4064 and by 75% for 10 μ M (**Fig. 1B and 1C**). Once again, 10 μ M of GW4064 led to the same inhibition as with IFN- α . Moreover, we observed less HDAg-positive cells following treatments (**Fig. 1D**).

The effect of GW4064 on HDV was also analyzed in PHH infected with HBV and superinfected with HDV. Following treatment with FXR ligand GW4064, a 44 % reduction of intracellular HDV RNAs levels was observed at 10 μ M (**Fig. S1A**). Western blot and IF analyses also showed a decrease of HDV antigens in infected PHH (**Fig. S1B, S1C and S1D**). The anti-HDV activity of GW4064 was slightly lower in PHH than in dHepaRG cells, most likely reflecting a much higher replication of HDV in PHH (28).

HBV infection was also monitored by measuring total intracellular HBV RNAs and HBeAg levels secreted in cell culture supernatants. As expected based on previous studies (20), GW4064 strongly inhibited both markers of HBV replication in either superinfected dHepaRG cells or PHH (**Fig. S2**).

Overall, these results showed an anti-HDV activity of the FXR ligand GW4064 both at the RNA and protein level in two relevant *in vitro* models of HBV/HDV superinfection.

FXR ligands inhibit early phases of HDV infection in dHepaRG cells and PHH monoinfected with HDV.

To further describe the inhibitory effect of FXR ligands on HDV infection, we analyzed the impact of FXR ligands whether treatment was initiated at early times post-infection or after the peak of HDV replication, to determine whether FXR modulation affected infection establishment or later phases of the HDV life cycle. To this end, HDV mono-

infection experiments were performed in dHepaRG cells thus freeing a potential effect of FXR ligands on HBV infection. Following infections, cells were treated at day 1 post-infection (early treatment) or at day 5 post-infection (late treatment). Moreover, to rule out putative off-target effects of GW4064, cells were treated for 10 days with three structurally different FXR ligands, a BA derivate (6-ECDCA), and two non-steroidal synthetic ligands (GW4064 and tropifexor). Quantification by RT-qPCR at the end of treatment showed that GW4064, 6-ECDCA and tropifexor reduced the amount of total intracellular HDV RNAs by around 50% following early treatment (**Fig. 2A**). A decrease in HDV RNAs was also observed after late treatment. However, this decrease was overall less pronounced and not significant with GW4064. For both early and late treatments, FXR ligands significantly decreased the level of FXR mRNA and strongly increased the level of BSEP mRNA as expected (**Fig. 2B and 2C**). As the different forms of viral RNAs produced in HDV-infected cells could not be discriminated by our RT-qPCR, we verified by northern blot analysis the effect of FXR ligands on genomic and antigenomic RNAs. Results showed that levels of both genomic and antigenomic RNAs were decreased following treatment with all three FXR ligands (**Fig. S3**). Similar experiments of early and late treatments were performed in PHH. Contrary to dHepaRG cells, an antiviral effect of FXR ligands was only observed when treatment was initiated at early phases of HDV infection. The maximal inhibition was obtained with tropifexor with a 60 % decrease of HDV RNAs compared to a 30 % decrease with GW4064. When infection was established, FXR ligands were not efficient to impede HDV replication (**Fig. S4**). As PHH maintain detoxification capacities, these differences may result from different kinetics of FXR ligands catabolism in these cells. Importantly, treatment did not significantly modify hepatocyte nuclear factor-4 (HNF4A) mRNA expression compared to untreated cells, suggesting that the evolution of the differentiation state of PHH was not strongly

affected by FXR ligands (**Fig. S5**). Together, these results showed that three FXR agonists displayed antiviral activity against HDV, especially on early HDV infection phases in two relevant *in vitro* models. An antiviral effect of a late treatment was only observed in dHepaRG cells. The use of three structurally different FXR ligands showed that anti-HDV activity of GW4064 was not the result of an off-target effect. Moreover, the inhibitory effect of FXR ligands did not require the presence of HBV.

Antiviral activity of FXR ligands is specific and relies on the presence of FXR.

FXR ligands used in these experiments, in particular GW4064 and tropifexor, are considered highly specific for FXR. However, to confirm that the antiviral activity of these molecules was indeed FXR-specific, we silenced FXR in HDV-monoinfected cells. We took advantage of a HepaRG cell line expressing an inducible Cas9 (described in **Fig. S6**) to use CRISPR-Cas9 technology to stably repress FXR expression. Two synthetic crRNA targeting distinct exons of the FXR gene were used. Transfection of either of the two guide RNAs led to a strong decrease in FXR protein level, indicating that both guides were efficient to block FXR protein synthesis (**Fig. 3A**). In line with our previous results, a 6-day treatment with GW4064 moderately, but significantly, reduced the amount of total intracellular HDV RNAs in non-transfected cells and in cells transfected with a control crRNA (**Fig. 3B**). In FXR-silenced cells, the inhibitory effect of GW4064 was either completely (case of guide#1) or greatly (case of guide#2) reverted, confirming that its anti-HDV activity was indeed dependent on FXR expression. To confirm these results, we also silenced FXR in dHepaRG cells coinfecting with HBV and HDV by using small interfering RNA (siRNA) technology. The antiviral effect of three FXR ligands was reverted in the presence of siRNA targeting FXR whose expression was decreased by more than 80% (**Fig. S7A and S7B**). The induction of BSEP expression was also reduced

in the presence of siFXR after FXR ligands treatment compared to siCTRL untreated condition (**Fig. S7C**). Partial or complete reversion of the antiviral impact of FXR ligands on HBV was also observed following FXR silencing (**Fig. S7D**). Overall these results demonstrated that inhibition of HDV markers induced by FXR ligands was dependent on the presence of FXR, its specific target.

FXR ligands strongly decrease the secretion of HDV particles in dHepaRG cells and PHH coinfecting with HBV and HDV.

Next, we wanted to evaluate the effect of FXR ligands on HDV particles secretion corresponding to the late step of the HDV life cycle. To this end, HBV/HDV coinfections were performed in dHepaRG cells. Following infection, cells were treated at day 1 (early treatment) or at day 5 post-infection (late treatment). Following a 10-day treatment, cells and supernatants were collected for further analyses. As previously observed in HDV-monoinfected cells, all three FXR ligands decreased by around 50% the amount of intracellular HDV RNAs following early treatment whereas after a late treatment, this decrease was lower or not significant (**Fig. 4A**). Analysis of secreted viral parameters showed that a decrease of secreted HDV RNAs in supernatants was observed following early treatment with FXR ligands by around 60%. In contrast to intracellular HDV RNAs, secreted HDV RNAs were reduced following a late treatment in the same proportions as early treatment (**Fig. 4B**). A decrease in total HBV RNAs and secreted HBV DNAs was reported by more than 50% after early and late treatments with FXR agonists (**Fig. 4C** and **4D**). As expected, a decrease of FXR mRNA and an induction of BSEP mRNA were observed following treatment with FXR agonists (**Fig. S8**). Overall, these results showed that treatment with FXR ligands affected the secretion step of the HDV life cycle, even when treatment was performed late at the peak of HDV replication.

FXR ligand GW4064 decreases specific infectivity of HDV particles.

Next, we wanted to determine the impact of FXR ligands on specific infectivity of secreted HDV particles. This was particularly important to look, since the continuous infection of naïve or already infected hepatocytes by HBs-bearing infectious HDV virions is thought to play a major role in HDV persistence in patients, as opposed to HBV for which persistence is a less dynamic process associated with long-lived cccDNA (30). To this end, HBV/HDV coinfection experiments were performed in dHepaRG cells according to the protocol depicted in **Fig. 5A**. Cells were treated for 10 days with either GW4064, IFN- α or a specific HBV-polymerase inhibitor (lamivudine). At the end of treatment, cells and supernatants of dHepaRG cells were collected for further analysis. First, western blot analysis of the levels of intracellular HDV antigens was performed to confirm the antiviral effect of FXR ligands. As previously observed, GW4064 and IFN- α treatment strongly decreased the amount of intracellular HDAg-S and HDAg-L, while lamivudine had no effect, as expected (**Fig. 5B**). Quantification of HDV RNA in supernatants by RT-qPCR revealed that secretion of HDV genomes decreased by 65 % following GW4064 treatment, and 52 % with IFN- α treatment (**Fig. 5C**). Of note, lamivudine slightly and unexpectedly stimulated HDV viral secretion through a mechanism that still needs to be clarified.

To determine the specific infectivity of secreted HDV, viral particles in supernatants were concentrated using PEG precipitation and naïve HuH7.5-NTCP cells were infected with the same viral genome equivalents for each condition. Six days post-infection, intracellular HDV RNA was quantified by RT-qPCR and HDV antigens production was evaluated by IF staining. Total intracellular HDV RNAs in HuH7.5-NTCP cells decreased by 98 % and 71% when cells were infected with supernatants from infected dHepaRG

cells treated with GW4064 and IFN- α , respectively (**Fig. 5D**). By contrast, treatment with lamivudine did not affect specific infectivity of HDV particles. Interestingly, when infecting naïve HuH7.5-NTCP cells with different inoculum (*i.e.* 100 and 500 vge per cell), a dose response was observed with supernatants from dHepaRG cells treated with either IFN- α , lamivudine or vehicle, whereas this was not the case for GW4064 (**Fig. 5E**). Finally, IF staining confirmed the RT-qPCR data as HDAg-positive cells could hardly be detected among HuH7.5-NTCP cells infected with supernatants from dHepaRG cells treated with GW4064 (**Fig. 5F**).

Supernatants were also subjected to isopycnic centrifugation on iodixanol density gradients. Fractions collected were tested for density, HDV RNA and HBV DNA by qPCR, HBsAg by ELISA and HDAg and HBsAg by western blot. No modification in the distribution and densities of fractions containing HDV RNA, HBV DNA, HDAg, HBsAg, was observed following treatment with GW4064, IFN- α and lamivudine, compared to untreated cells (**Fig. S9**). Similar experiments were performed with FXR ligands 6-ECDCA and tropifexor to confirm results obtained with GW4064. Following infection of naïve HuH7.5-NTCP cells with viruses produced in dHepaRG cells treated with 6-ECDCA and tropifexor, a decrease of intracellular HDV RNAs by more than 95 % was also observed, indicating that the specific infectivity of secreted HDV particles was affected by all three FXR ligands used in this study (**Fig. S10A and S10B**). A comparable decrease of infectivity was observed when naïve dHepaRG cells were infected with HDV viruses produced in the same conditions of treatment (**Fig. S10C**). Altogether, these results showed that FXR ligands not only decreased secretion of HDV particles in infected dHepaRG cells but also impaired their specific infectivity.

Discussion

This study shows that, in the most relevant *in vitro* models of HDV infection, treatment with FXR ligands moderately reduces early steps of HDV intracellular replication, more efficiently inhibits secretion of HDV virions and drastically inhibits the specific infectivity of secreted viral particles. Target engagement was confirmed by the use of several ligands with different chemical structures and FXR loss of function experiments.

In HDV monoinfected dHepaRG cells, the amount of genomic and antigenomic HDV RNA, which are key markers of HDV replication, was reduced by the treatment with FXR ligands. This demonstrates that, at least for the HDV genome replication steps, the inhibitory effect of FXR ligands is unrelated to their anti-HBV activity, which has been previously described (20,21). In HBV/HDV coinfection models, it is shown that FXR ligands induced a decrease in HDV RNA secretion. This impaired secretion of hepatitis delta virions may result from the decrease of all markers of HDV replication (HDV RNAs and proteins), combined with the inhibition of HBs synthesis, not excluding other mechanisms that remain to be identified.

One major impact of FXR activation is the pronounced decrease in specific infectivity (by more than 95 %) of virions produced by coinfecting dHepaRG cells. HDV RNA-containing particles were indeed poorly efficient to infect and/or initiate viral replication in naive HuH7.5-NTCP cells, suggesting key modifications of virion composition following treatment. No shift in the density of RNA-, HDAg- or HBs-containing fractions secreted upon FXR engagement could be observed but a detailed analysis of virion composition and structure is warranted (*i.e.* proteomic, lipidomic, atomic-force microscopy). Importantly, this reduction of specific infectivity obtained with GW4064, 6-ECDC and tropifexor was superior to that obtained with the SoC IFN- α .

One limitation of the study is that all experiments were performed using a unique HDV strain of genotype 1 with a particular history (31). This strain is commonly used in HDV research, however it would be of great interest to study the antiviral effect of FXR ligands on other HDV genotypes.

FXR belongs to the NR superfamily, a group of transcription factors sharing a common modular structure that includes a DNA-binding domain and a ligand-binding domain. Binding of ligands on FXR may result in FXR activation and modulation of FXR target genes expression, in modifications of FXR conformation leading to either promotion or destabilization of interactions with nucleic acids or protein partners and finally in repression of FXR expression via a negative feedback loop. HDV RNAs, HDV Ag-S and host components associate to form HDV viral replication/transcription complexes. In particular, it was shown that host DNA-dependent RNA polymerase II could be recruited onto HDV RNA genome and drive transcription, thus indicating that HDV can hijack host factors known to interact with dsDNA and not dsRNA (32). To our knowledge, FXR activation does not directly modulate the expression of DNA-dependent RNA polymerase II but it is well established that ligand binding induces a conformational change of nuclear receptors, leading to the recruitment of various coactivators, some of them with acetylase and methylase activities. Histone acetylation and methylation status is then modified by these coactivators with consequences on the transcription of target genes. Whether this could apply to the regulation of HDV transcription remains to be explored, as the regulation of RNA polymerase II on the HDV genome is far from being fully understood. However, one can speculate that FXR may interact or interfere with viral or cellular components within HDV replication complexes, and that this interaction may be modified by FXR ligands.

Alternatively, FXR activation by ligands may specifically modulate expression of genes involved in pathways playing a key role in the HDV life cycle. Such modulations may lead to altered replication and transcription of the HDV genome and/or modifications of the structure and composition of secreted particles during virion assembly. FXR is an essential regulator of several liver metabolic pathways, its role in regulating lipid metabolism (in particular BA and lipoprotein metabolism) and glucose metabolism being extensively studied. However, its role is not limited to these pathways, as FXR has also been linked to the regulation of liver regeneration and innate immunity (17,33). Cellular pathways essential for the HDV life cycle are still poorly known to date. Recently, a screening based on RNA interference identified several cellular pathways involved in HDV replication such as HIF-1 signalling pathway, pyrimidine biosynthesis, insulin resistance or glycosaminoglycan biosynthesis (34). Protein prenylation pathway is also known to play a key role during HDV virion assembly as farnesylation of HDAg-L by cellular farnesyl-transferases favors HDAg-L localization to the ER and association with HBsAg. Interestingly, some links exist between prenylation and BA pathways. Besides geranylgeranyl, farnesyl can also be transformed into squalene, an essential biochemical precursor for steroids (including cholesterol and BA) or farnesol. Farnesol was the first ligand identified for FXR (35) but, following the identification of BA as new FXR ligands, studies on relationships between FXR and prenylation pathway were given less priority. Given the major impact of FXR ligands on HDV virion infectivity, studying the impact of FXR activation on HDAg-L may be of great interest. Moreover, overexpression of HDAg-L has also been shown to inhibit HDV viral replication (11), and FXR-induced putative modulations of HDAg-L activity might also interfere with the replication step of HDV cycle

In conclusion, our results revealed that FXR agonists inhibit early steps of intracellular HDV genome replication in *in vitro* infected dHepaRG and PHH, with an antiviral activity comparable to that of IFN- α . In HBV/HDV coinfecting cells, FXR ligation decreases HDV secretion and even more significantly reduces the specific infectivity of secreted HDV virions, leading altogether to an antiviral phenotype far superior to that obtained with IFN- α , the current SoC in HDV patients. After HBV, HDV is the second hepatotropic virus that appears to be very sensitive to therapeutic FXR agonization, which suggests that this nuclear receptor may be broadly involved in host antiviral responses. The majority of studies focus on FXR metabolic functions and a more detailed analysis of mechanisms underlying FXR antiviral activity has to be pursued.

To date the therapeutic options for patients infected with HDV are limited to Peg-IFN- α and bulevirtide, an entry inhibitor. Other molecules are currently under evaluation: Peg-IFN- λ 1, lonafarnib, a prenylation inhibitor that impairs HDV secretion, and REP 2139, a nucleic acid polymer that inhibits HBs, HBV and HDV secretion. Combined therapies will likely be necessary to achieve a sustained virological response in the majority of patients. As constant reinfection of hepatocytes is thought to play a major role in HDV persistence, the strong inhibition of virion production and spreading following treatment with FXR ligands opens promising therapeutic perspectives for these molecules in the treatment of hepatitis delta. FXR is an attractive target for the development of antiviral molecules as some FXR ligands have already been approved for patients with primary biliary cholangitis or are currently in clinical evaluation in patients with non-alcoholic steatohepatitis (NASH) (36). Moreover, one FXR ligand is currently in a phase II clinical trial in patients with chronic HBV infection (Clinical Trial identifiers NCT04365933 and NCT04465916). In this context, the clinical evaluation of

FXR modulators in HBV/HDV coinfecting patients, alone or in combination, could be a successful strategy.

References

1. Miao Z, Zhang S, Ou X, Li S, Ma Z, Wang W, et al. Estimating the Global Prevalence, Disease Progression, and Clinical Outcome of Hepatitis Delta Virus Infection. *J. Infect. Dis.* 2020;221:1677–1687.
2. Alfaiate D, Clément S, Gomes D, Goossens N, Negro F. Chronic hepatitis D and hepatocellular carcinoma: A systematic review and meta-analysis of observational studies. *J. Hepatol.* 2020;73:533–539.
3. Stockdale AJ, Kreuels B, Henrion MYR, Giorgi E, Kyomuhangi I, de Martel C, et al. The global prevalence of hepatitis D virus infection: Systematic review and meta-analysis. *J. Hepatol.* 2020;73:523–532.
4. Chen H-Y, Shen D-T, Ji D-Z, Han P-C, Zhang W-M, Ma J-F, et al. Prevalence and burden of hepatitis D virus infection in the global population: a systematic review and meta-analysis. *Gut.* 2019;68:512–521.
5. Lempp FA, Ni Y, Urban S. Hepatitis delta virus: insights into a peculiar pathogen and novel treatment options. *Nat. Rev. Gastroenterol. Hepatol.* 2016;13:580–589.
6. Koh C, Heller T, Glenn JS. Pathogenesis of and New Therapies for Hepatitis D. *Gastroenterology.* 2019;156:461-476.e1.
7. Kang C, Syed YY. Bulevirtide: First Approval. *Drugs.* 2020;80:1601–1605.
8. Lucifora J, Delphin M. Current knowledge on Hepatitis Delta Virus replication. *Antiviral Res.* 2020;179:104812.
9. Wong SK, Lazinski DW. Replicating hepatitis delta virus RNA is edited in the

nucleus by the small form of ADAR1. *Proc. Natl. Acad. Sci. U. S. A.* 2002;99:15118–15123.

10. Hwang SB, Lai MM. Isoprenylation mediates direct protein-protein interactions between hepatitis large delta antigen and hepatitis B virus surface antigen. *J. Virol.* 1993;67:7659–7662.
11. Chao M, Hsieh SY, Taylor J. Role of two forms of hepatitis delta virus antigen: evidence for a mechanism of self-limiting genome replication. *J. Virol.* 1990;64:5066–5069.
12. Ryu WS, Netter HJ, Bayer M, Taylor J. Ribonucleoprotein complexes of hepatitis delta virus. *J. Virol.* 1993;67:3281–3287.
13. Sureau C, Negro F. The hepatitis delta virus: Replication and pathogenesis. *J. Hepatol.* 2016;64:S102–S116.
14. Yan H, Zhong G, Xu G, He W, Jing Z, Gao Z, et al. Sodium taurocholate cotransporting polypeptide is a functional receptor for human hepatitis B and D virus. *eLife* [Internet]. 2012 [cited 2019 Sep 3];1. Available from: <https://elifesciences.org/articles/00049>
15. Ni Y, Lempp FA, Mehrle S, Nkongolo S, Kaufman C, Fälth M, et al. Hepatitis B and D viruses exploit sodium taurocholate co-transporting polypeptide for species-specific entry into hepatocytes. *Gastroenterology.* 2014;146:1070–1083.
16. Yan H, Peng B, Liu Y, Xu G, He W, Ren B, et al. Viral Entry of Hepatitis B and D Viruses and Bile Salts Transportation Share Common Molecular Determinants on Sodium Taurocholate Cotransporting Polypeptide. *J. Virol.* 2014;88:3273–3284.
17. Lefebvre P, Cariou B, Lien F, Kuipers F, Staels B. Role of Bile Acids and Bile Acid Receptors in Metabolic Regulation. *Physiol. Rev.* 2009;89:147–191.
18. Ramière C, Scholtès C, Diaz O, Icard V, Perrin-Cocon L, Trabaud M-A, et al. Transactivation of the hepatitis B virus core promoter by the nuclear receptor FXR α .

J. Virol. 2008;82:10832–10840.

19. Oehler N, Volz T, Bhadra OD, Kah J, Allweiss L, Giersch K, et al. Binding of hepatitis B virus to its cellular receptor alters the expression profile of genes of bile acid

metabolism: Oehler, Volz et al. Hepatology. 2014;60:1483–1493.

20. Radreau P, Porcherot M, Ramière C, Mouzannar K, Lotteau V, André P. Reciprocal regulation of farnesoid X receptor α activity and hepatitis B virus replication in differentiated HepaRG cells and primary human hepatocytes. FASEB J. Off. Publ. Fed. Am. Soc. Exp. Biol. 2016;30:3146–3154.

21. Mouzannar K, Fusil F, Lacombe B, Ollivier A, Ménard C, Lotteau V, et al. Farnesoid X receptor- α is a proviral host factor for hepatitis B virus that is inhibited by ligands in vitro and in vivo. FASEB J. Off. Publ. Fed. Am. Soc. Exp. Biol. 2019;33:2472–2483.

22. Erken R, Andre P, Roy E, Kootstra N, Barzic N, Girma H, et al. Farnesoid X receptor agonist for the treatment of chronic hepatitis B: A safety study. J. Viral Hepat. 2021;28:1690–1698.

23. Sureau C. The Use of Hepatocytes to Investigate HDV Infection: The HDV/HepaRG Model [Internet]. In: Maurel P, editor. Hepatocytes. Totowa, NJ: Humana Press; 2010 [cited 2019 Sep 3]. p. 463–473. Available from: http://link.springer.com/10.1007/978-1-60761-688-7_25

24. Ladner SK, Otto MJ, Barker CS, Zaifert K, Wang GH, Guo JT, et al. Inducible expression of human hepatitis B virus (HBV) in stably transfected hepatoblastoma cells: a novel system for screening potential inhibitors of HBV replication. Antimicrob. Agents Chemother. 1997;41:1715–1720.

25. Gripon P, Rumin S, Urban S, Le Seyec J, Glaise D, Cannie I, et al. Infection of a human hepatoma cell line by hepatitis B virus. Proc. Natl. Acad. Sci. U. S. A. 2002;99:15655–15660.

26. Alfaiate D, Lucifora J, Abeywickrama-Samarakoon N, Michelet M, Testoni B, Cortay J-C, et al. HDV RNA replication is associated with HBV repression and interferon-stimulated genes induction in super-infected hepatocytes. *Antiviral Res.* 2016;136:19–31.
27. Lecluyse EL, Alexandre E. Isolation and culture of primary hepatocytes from resected human liver tissue. *Methods Mol. Biol.* Clifton NJ. 2010;640:57–82.
28. Michelet M, Alfaiate D, Chardès B, Pons C, Faure-Dupuy S, Engleitner T, et al. Inducers of NF- κ B pathways impair hepatitis delta virus replication and strongly decrease progeny infectivity in vitro. *JHEP Rep.* [Internet]. [cited 2022 Jan 17]; Available from: <https://doi.org/10.1016/j.jhepr.2021.100415>
29. Wang L, Lee Y-K, Bundman D, Han Y, Thevananther S, Kim CS, et al. Redundant pathways for negative feedback regulation of bile acid production. *Dev. Cell.* 2002;2:721–731.
30. Zhang Z, Urban S. New insights into HDV persistence: The role of interferon response and implications for upcoming novel therapies. *J. Hepatol.* 2021;74:686–699.
31. Kuo MY, Goldberg J, Coates L, Mason W, Gerin J, Taylor J. Molecular cloning of hepatitis delta virus RNA from an infected woodchuck liver: sequence, structure, and applications. *J. Virol.* 1988;62:1855–1861.
32. Mentha N, Clément S, Negro F, Alfaiate D. A review on hepatitis D: From virology to new therapies. *J. Adv. Res.* 2019;17:3–15.
33. Fiorucci S, Biagioli M, Zampella A, Distrutti E. Bile Acids Activated Receptors Regulate Innate Immunity. *Front. Immunol.* [Internet]. 2018 [cited 2019 Sep 4];9. Available from: <https://www.frontiersin.org/article/10.3389/fimmu.2018.01853/full>
34. Verrier ER, Weiss A, Bach C, Heydmann L, Turon-Lagot V, Kopp A, et al. Combined small molecule and loss-of-function screen uncovers estrogen receptor alpha and CAD

as host factors for HDV infection and antiviral targets. *Gut*. 2020;69:158–167.

35. Forman B. Identification of a nuclear receptor that is activated by farnesol metabolites. *Cell*. 1995;81:687–693.

36. Sumida Y, Yoneda M, Ogawa Y, Yoneda M, Okanoue T, Nakajima A. Current and new pharmacotherapy options for non-alcoholic steatohepatitis. *Expert Opin. Pharmacother*. 2020;21:953–967.

Figure Legends

Figure 1. FXR ligand GW4064 decreases the levels of intracellular HDV RNAs and proteins in HBV-infected dHepaRG superinfected with HDV. Differentiated HepaRG cells were infected with HBV at a MOI of 100 vge per cell and 7 days later with HDV at a MOI of 10 vge per cell. Three days post-HDV infection, cells were treated with 1, 5 or 10 μ M of GW4064, IFN- α (1000 IU/mL) or not. Cells were harvested 10 days post-treatment for cellular RNA and protein extraction or fixed with formaldehyde for immunofluorescence analyses. Intracellular HDV RNAs were quantified (A). Results are the mean \pm SD of three experiments each performed with three biological replicates. Student's t-test * $p < 0.05$, ** $p < 0.01$, *** $p < 0.001$. Analysis of the levels of HDAG by western blot analyses were performed using anti-HDAG antibodies and anti-B-tubulin antibodies as a loading control (B). Densitometry analyses are presented as ratios of HDAGs normalized to the levels of B-tubulin (C). Immunofluorescence analyses were performed using anti-HDAG antibodies and nuclei DAPI staining (D). Scale bar: 200 μ m.

Figure 2. FXR ligands inhibit early and late phases of HDV infection in HDV-monoinfected dHepaRG cells. Differentiated HepaRG cells were infected with HDV at a MOI of 10 vge per cell. Cells were treated with 10 μ M of GW4064 or 6-ECDCA or 0.1 μ M of tropifexor, 1 day post-infection for early treatment and 5 days post-infection for late treatments. Cells were harvested 10 days post-treatment. Total cellular RNAs were extracted and intracellular HDV RNAs (A), FXR mRNA (B) and BSEP mRNA (C) were quantified by RT-qPCR. Results are the mean \pm SD of three experiments each performed with 3 biological replicates. Data are normalized to untreated conditions for early and late treatments. Student's t-test, * p <0.05, ** p <0.01, *** p <0.001, ns: not significant.

Figure 3. FXR ligands decrease the levels of intracellular HDV RNAs in an FXR-dependent manner. dHepaRG-TR-Cas9 cells were transfected twice with indicated RNA guides 4 days and 1 day before infection with HDV at a MOI of 25 vge per cell. From day 3 to day 9 post-infection, cells were treated with 10 μ M of GW4064 or vehicle. Cells were harvested at day 9 post-infection. (A) Levels of FXR proteins were analyzed by Western Blot. GAPDH detection was used as a loading control. (B) Total cellular RNAs were extracted and the levels of total intracellular HDV RNAs were quantified by RT-qPCR. Results are the mean \pm SD of three experiments each performed with three biological replicates. Data are normalized to the untreated cells for each condition of transfection. 2-way ANOVA, ** p < 0.01, ns: not significant. NT: non-transfected.

Figure 4. FXR ligands inhibit secretion of HDV RNA in dHepaRG cells coinfecting with HBV and HDV. dHepaRG cells were coinfecting with HBV and HDV using 100 and 10 vge per cell, respectively. Cells were treated with 10 μ M of GW4064 or 6-ECDCA or

0.1 μ M of tropifexor, 1 day post-infection for early treatment and 5 days post-infection for late treatment. Cells and supernatants were harvested 10 days post-treatment. Total cellular RNAs and viral nucleic acids in supernatants were extracted. Intracellular (A) and secreted (B) HDV RNAs were quantified by RT-qPCR. Intracellular HBV RNAs (C) and secreted HBV DNA (D) were also quantified by RT-qPCR and qPCR, respectively. Results are the mean \pm SD of three experiments each performed with 3 biological replicates. Data are normalized to the untreated conditions for early and late treatments. Student's t-test, * $p < 0.05$, ** $p < 0.01$, *** $p < 0.001$ ns: not significant.

Figure 5. GW4064 reduces the infectivity of HDV particles. dHepaRG cells were coinfecting with HBV and HDV with 500 vge per cell for HBV and 50 vge per cell for HDV. Cells were treated or not 3 days later with GW4064 (10 μ M), IFN- α (500 IU/mL) or lamivudine (LAM, 10 μ M) for 10 days. (A) Schematic representation of experimental procedure. (B) dHepaRG cells were collected and the level of intracellular HDAg was analyzed by western blot. (C) Supernatants of infected dHepaRG cells were collected, concentrated by PEG precipitation and the levels of extracellular HDV RNAs (called HDV-2P for second passage) were assessed by qRT-PCR analyses. (D-F) Naïve HuH7.5-NTCP cells were infected with the different concentrated supernatants (HDV-2P) with (D) 500 vge cell or (E) the indicated vge/cell. Six days later, (D, E) levels of intracellular HDV RNAs were assessed by RT-qPCR analyses; (F) cells were stained with DAPI and anti-HDAg antibodies. Scale bar: 200 μ m. Results of RT-qPCR are the mean \pm SD of three independent experiments each performed with three biological replicates. Student's t-test, ** $p < 0.01$, *** $p < 0.001$, ns: not significant.

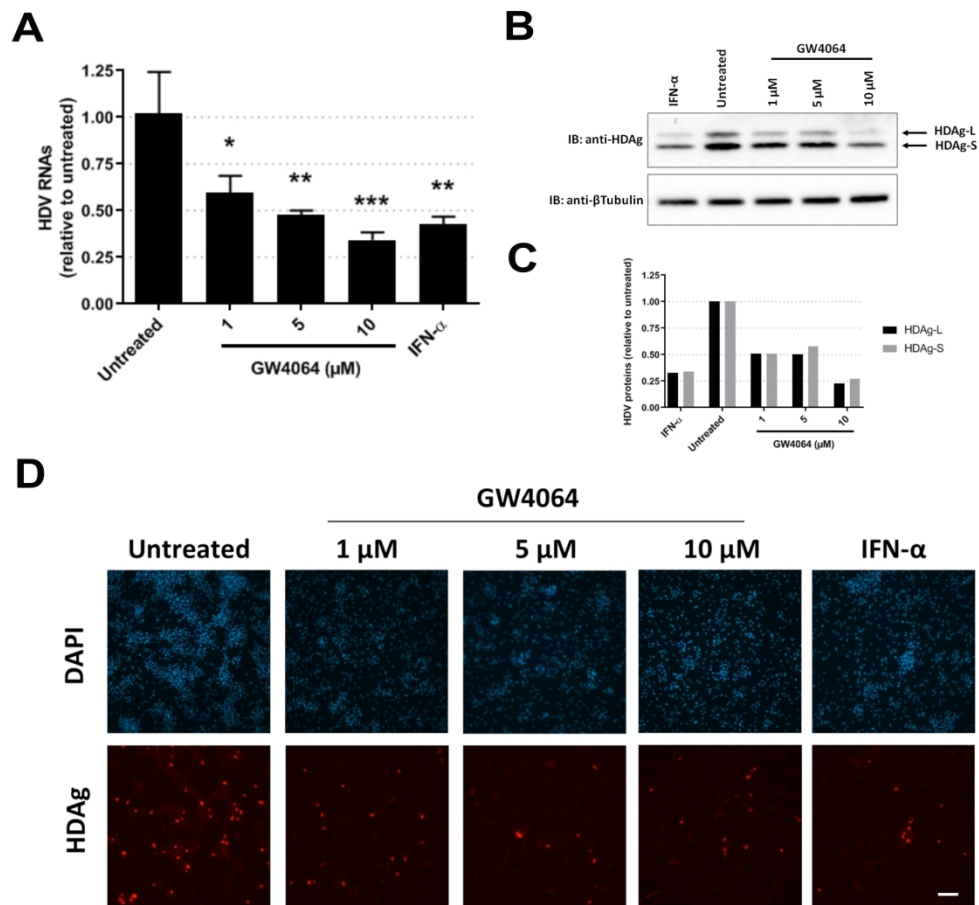


Figure 1. FXR ligand GW4064 decreases the levels of intracellular HDV RNAs and proteins in HBV-infected dHepaRG superinfected with HDV. Differentiated HepaRG cells were infected with HBV at a MOI of 100 vge per cell and 7 days later with HDV at a MOI of 10 vge per cell. Three days post-HDV infection, cells were treated with 1, 5 or 10 μ M of GW4064, IFN- α (1000 IU/mL) or not. Cells were harvested 10 days post-treatment for cellular RNA and protein extraction or fixed with formaldehyde for immunofluorescence analyses. Intracellular HDV RNAs were quantified (A). Results are the mean \pm SD of three experiments each performed with three biological replicates. Student's t-test * p < 0.05, ** p < 0.01, *** p < 0.001. Analysis of the levels of HDAg by western blot analyses were performed using anti-HDAg antibodies and anti- β -tubulin antibodies as a loading control (B). Densitometry analyses are presented as ratios of HDAGs normalized to the levels of β -tubulin (C). Immunofluorescence analyses were performed using anti-HDAg antibodies and nuclei DAPI staining (D). Scale bar: 200 μ m.

209x196mm (300 x 300 DPI)

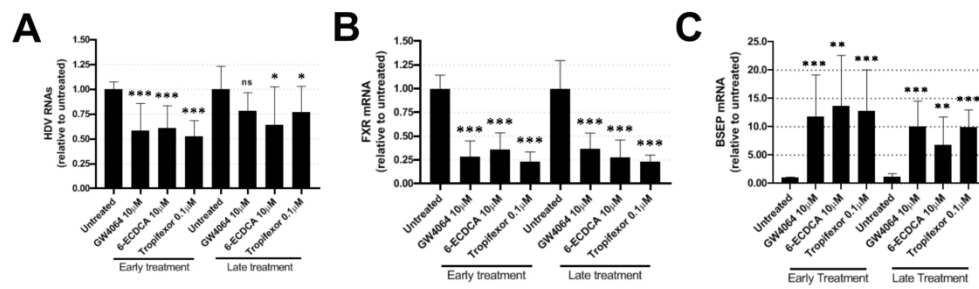


Figure 2. FXR ligands inhibit early and late phases of HDV infection in HDV-monoinfected dHepaRG cells. Differentiated HepaRG cells were infected with HDV at a MOI of 10 vge per cell. Cells were treated with 10 μ M of GW4064 or 6-ECDCA or 0.1 μ M of tropifexor, 1 day post-infection for early treatment and 5 days post-infection for late treatments. Cells were harvested 10 days post-treatment. Total cellular RNAs were extracted and intracellular HDV RNAs (A), FXR mRNA (B) and BSEP mRNA (C) were quantified by RT-qPCR. Results are the mean \pm SD of three experiments each performed with 3 biological replicates. Data are normalized to untreated conditions for early and late treatments. Student's t-test, *p<0.05, **p<0.01, ***p<0.001, ns: not significant.

209x65mm (300 x 300 DPI)

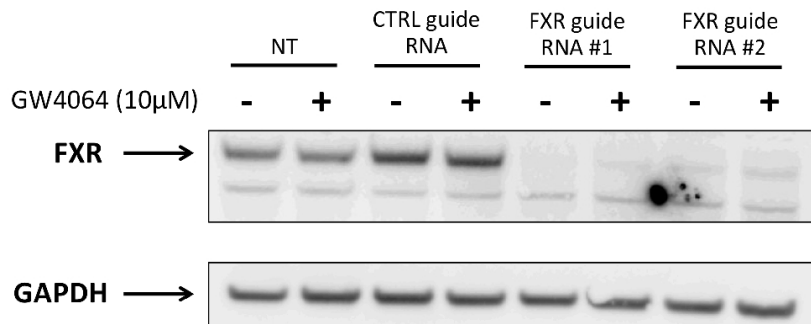
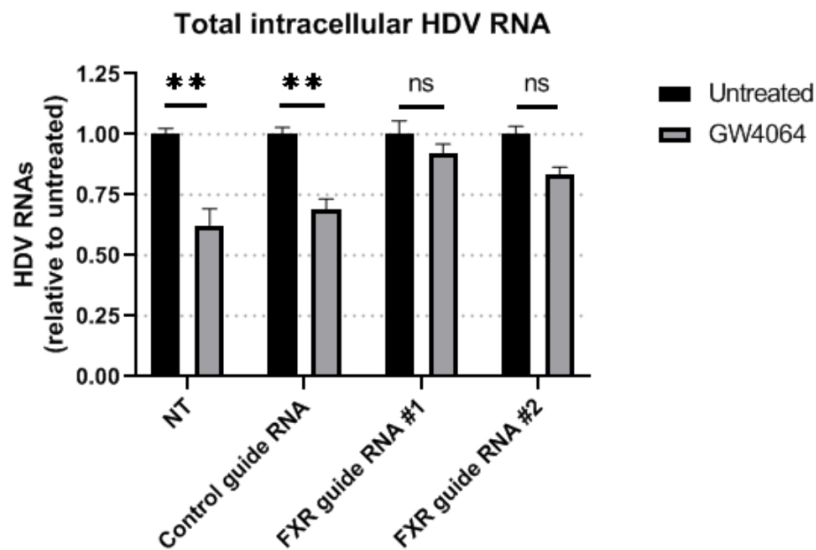
A**B**

Figure 3. FXR ligands decrease the levels of intracellular HDV RNAs in an FXR-dependent manner. dHepaRG-TR-Cas9 cells were transfected twice with indicated RNA guides 4 days and 1 day before infection with HDV at a MOI of 25 vge per cell. From day 3 to day 9 post-infection, cells were treated with 10 μ M of GW4064 or vehicle. Cells were harvested at day 9 post-infection. (A) Levels of FXR proteins were analyzed by Western Blot. GAPDH detection was used as a loading control. (B) Total cellular RNAs were extracted and the levels of total intracellular HDV RNAs were quantified by RT-qPCR. Results are the mean \pm SD of three experiments each performed with three biological replicates. Data are normalized to the untreated cells for each condition of transfection. 2-way ANOVA, ** $p < 0.01$, ns: not significant. NT: non-transfected.

94x120mm (300 x 300 DPI)

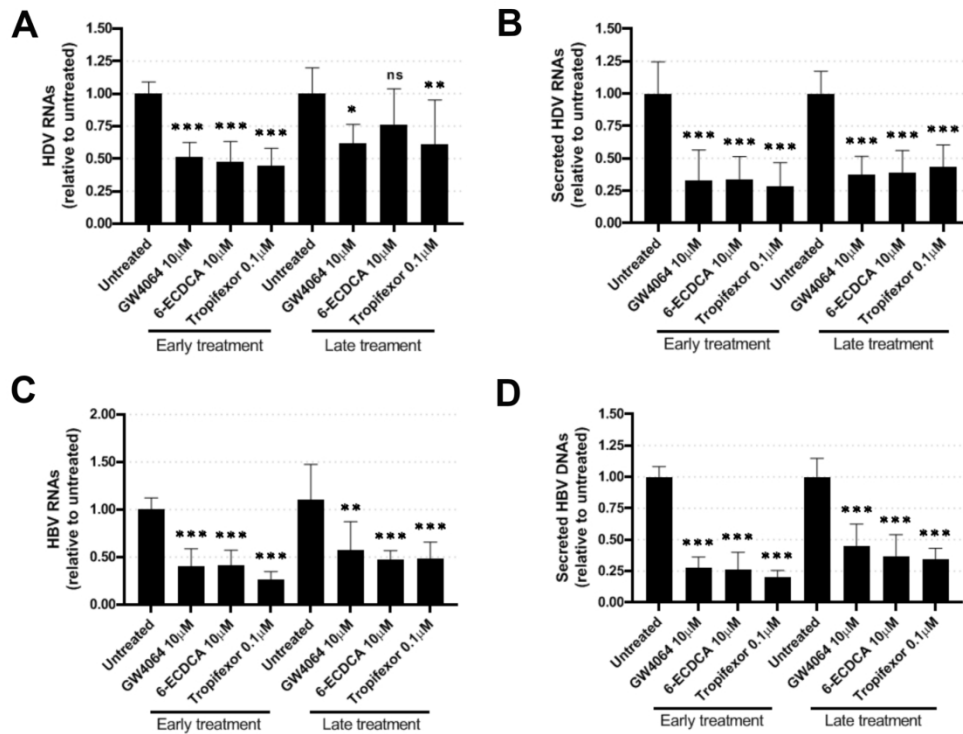


Figure 4. FXR ligands inhibit secretion of HDV RNA in dHepaRG cells coinfecting with HBV and HDV. dHepaRG cells were coinfecting with HBV and HDV using 100 and 10 vge per cell, respectively. Cells were treated with 10 μ M of GW4064 or 6-ECDCA or 0.1 μ M of tropicifexor, 1 day post-infection for early treatment and 5 days post-infection for late treatment. Cells and supernatants were harvested 10 days post-treatment. Total cellular RNAs and viral nucleic acids in supernatants were extracted. Intracellular (A) and secreted (B) HDV RNAs were quantified by RT-qPCR. Intracellular HBV RNAs (C) and secreted HBV DNA (D) were also quantified by RT-qPCR and qPCR, respectively. Results are the mean \pm SD of three experiments each performed with 3 biological replicates. Data are normalized to the untreated conditions for early and late treatments. Student's t-test, * p <0.05, ** p <0.01, *** p <0.001 ns: not significant.

169x127mm (300 x 300 DPI)

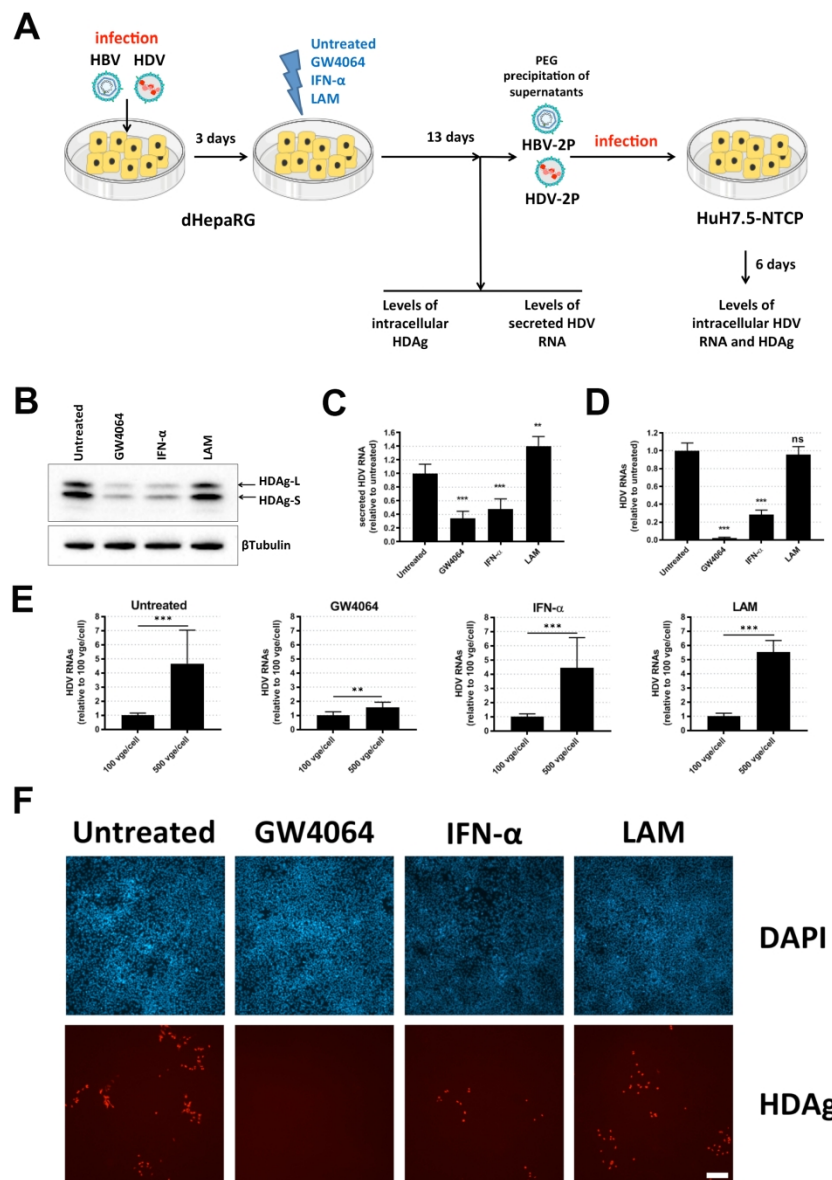


Figure 5. GW4064 reduces the infectivity of HDV particles. dHepaRG cells were coinfected with HBV and HDV with 500 vge per cell for HBV and 50 vge per cell for HDV. Cells were treated or not 3 days later with GW4064 (10 μ M), IFN- α (500 IU/mL) or lamivudine (LAM, 10 μ M) for 10 days. (A) Schematic representation of experimental procedure. (B) dHepaRG cells were collected and the level of intracellular HDV RNA was analyzed by western blot. (C) Supernatants of infected dHepaRG cells were collected and the level of extracellular HDV RNAs (called HDV-2P for second passage) were assessed by qRT-PCR analyses. (D-F) Naïve HuH7.5-NTCP cells were infected with the different concentrated supernatants (HDV-2P) with (D) 500 vge/cell or (E) the indicated vge/cell. Six days later, (D, E) levels of intracellular HDV RNAs were assessed by RT-qPCR analyses; (F) cells were stained with DAPI and anti-HDV antibodies. Scale bar: 200 μ m. Results of RT-qPCR are the mean \pm SD of three independent experiments each performed with three biological replicates. Student's t-test, ** p < 0.01, *** p < 0.001, ns: not significant.

195x274mm (300 x 300 DPI)

Supplementary methods

Nucleic acid quantification

Total intracellular RNAs were extracted by using the NucleoSpin RNA II kit according to the manufacturer's instructions (Macherey-Nagel). DNAs and RNAs from HBV or HDV particles were isolated from cell supernatants by using the NucleoSpin RNA Virus kit (Macherey-Nagel) according to the manufacturer's instructions. RNA was reverse-transcribed using either High-Capacity RNA-to-cDNA kit (ThermoFisher Scientific) or Maxima RT (Life Technologies). Quantitative PCR for HDV and HBV were performed as previously described (1,2). FXR and BSEP mRNAs were quantified by qPCR as previously described (3). HNF4A mRNA was quantified by using the following primers: 5'-CGTGGAGGCAGGGAGAATGCGA-3' and 5'-TTCTGATGGGGACGTGTCATTGC-3'. Statistical analyses were performed using Student's t-test: * $p < 0.05$, ** $p < 0.01$, *** $p < 0.001$, ns: not significant.

Northern blot for detection of HDV genomic and antigenomic RNAs was essentially performed as previously described (2). Briefly, purified RNA was denatured at 50°C for one hour with glyoxal (Life Technologies), subjected to electrophoresis through a phosphate 1.2% agarose gel and transferred to a nylon membrane (Amersham Np, GE). Membrane-bound RNA was hybridized to digoxigenin(DIG)-labeled HDV-specific probes. Quantitative analysis of HDV RNA was achieved by phosphorimager scanning (Typhoon Fla 9500, GE); 18S and 28S rRNA detection was used as loading control.

ELISA

Commercial immunoassay kits (Autobio Diagnostics Co., China) were used for HBsAg and HBeAg quantification in cell culture supernatants. Results are presented as a ratio to

a control sample, described for each experiment. Cut-offs for these ELISA were 0.05 IU/mL for HBsAg and 0.1 PEIU/mL for HBeAg.

Western blotting

For the detection of FXR protein by western blot, cells were lysed by using buffer containing 10 mM HEPES, 10mM NaOH (pH 7.5), 10 mM KCl, 1.5 mM MgCl₂, 0.3% NP40, protease inhibitor mixture cocktail (P8340-Merck) and Pierce™ universal nuclease for cell lysis (#88701, Thermo Fisher Scientific). Samples were then diluted with 4X Laemmli sample buffer (Biorad, #1610747) and supplemented with 1mM dithiothreitol. Mouse anti-FXR (clone A9033A, ThermoFisher Scientific) and anti-GAPDH (clone 1E6D9, Proteintech) antibodies were used, followed by horseradish peroxidase (HRP) detection with SuperSignal™ West Pico or Femto chemiluminescent substrate (Thermo Fisher Scientific) according to manufacturer's instructions. HRP signal detection was determined electronically using the Syngene PXi Image system (Ozyme).

For the detection of HDV antigens, cells were washed with Phosphate buffered saline (PBS) and harvested in RIPA lysis buffer (Tris-HCl pH 7.5 10mM, NaCl 140mM, EDTA 1mM, EGTA 0.5mM, 1% Triton X100, 0.1% SDS, 0.1% Na-Deoxycholate) containing protease inhibitors (Protein Cocktail Inhibitors from Sigma-Aldrich). Clarified lysates were subjected to SDS-PAGE and Western Blot transfer onto nitrocellulose membranes using the iBlot2 apparatus according to the manufacturer (Thermofisher Scientific). The polyclonal anti-HDAg serum, obtained by rabbit immunization (with a proprietary strategy), was a kind gift from Janssen. Anti-human β Tubulin was purchased from Abcam and used as a loading control. Detection was performed with Gel Doc XR p System (BioRad) and images were analyzed with ImageJ software.

Anti-HBsAg (H166), used for HBs detection in gradient fractions, has been previously described (4).

The references of antibodies used in this study are provided in Supplementary Table 1.

Immunofluorescence

Immunofluorescence (IF) experiments were performed as previously described (2). Cells were fixated with formaldehyde 4% and permeabilized by Triton 0.1%. Nuclei were stained with 4,6-diamidino-2-phenylindole (DAPI). The anti-HDAg antibody used was the same as for western blots. Secondary antibody used was goat anti-human Alexa Fluor 555 (Invitrogen). Images were obtained by epifluorescence microscopy (Nikon eclipse TE2000-E; Nikon).

siRNA transfections

siRNA transfections into dHepaRG cells were performed using Lipofectamine RNAiMAX (ThermoFisher Scientific) according to manufacturer's guidelines. siCTRL (ON-TARGETplus Non-targeting pool) and siFXR (ON-TARGETplus Human NR1H4 siRNA SMART pool) were purchased from Dharmacon (Horizon Discovery, Cambridge, UK).

Supplementary references

1. Lucifora J, Xia Y, Reisinger F, Zhang K, Stadler D, Cheng X, et al. Specific and nonhepatotoxic degradation of nuclear hepatitis B virus cccDNA. *Science*. 2014;343:1221–1228.
2. Alfaiate D, Lucifora J, Abeywickrama-Samarakoon N, Michelet M, Testoni B, Cortay J-C, et al. HDV RNA replication is associated with HBV repression and interferon-

stimulated genes induction in super-infected hepatocytes. *Antiviral Res.* 2016;136:19–31.

3. Mouzannar K, Fusil F, Lacombe B, Ollivier A, Ménard C, Lotteau V, et al. Farnesoid X receptor- α is a proviral host factor for hepatitis B virus that is inhibited by ligands in vitro and in vivo. *FASEB J. Off. Publ. Fed. Am. Soc. Exp. Biol.* 2019;33:2472–2483.
4. Chen YC, Delbrook K, Dealwis C, Mimms L, Mushahwar IK, Mandecki W. Discontinuous epitopes of hepatitis B surface antigen derived from a filamentous phage peptide library. *Proc. Natl. Acad. Sci. U. S. A.* 1996;93:1997–2001.

Supplementary Table 1

Antibodies	Application	Description	Source	Catalog/Clone number
FXR	WB	Mouse monoclonal	Thermo Fisher Scientific	clone A9033A
GAPDH	WB	Mouse monoclonal	Proteintech	clone 1E6D9
HDAg	WB, IF	Rabbit polyclonal	Janssen	proprietary strategy
β Tubulin	WB	Rabbit polyclonal	Abcam	ab15568
HBsAg	WB	Mouse monoclonal	Abbott Laboratories	H166

Supplementary figures

Figure S1

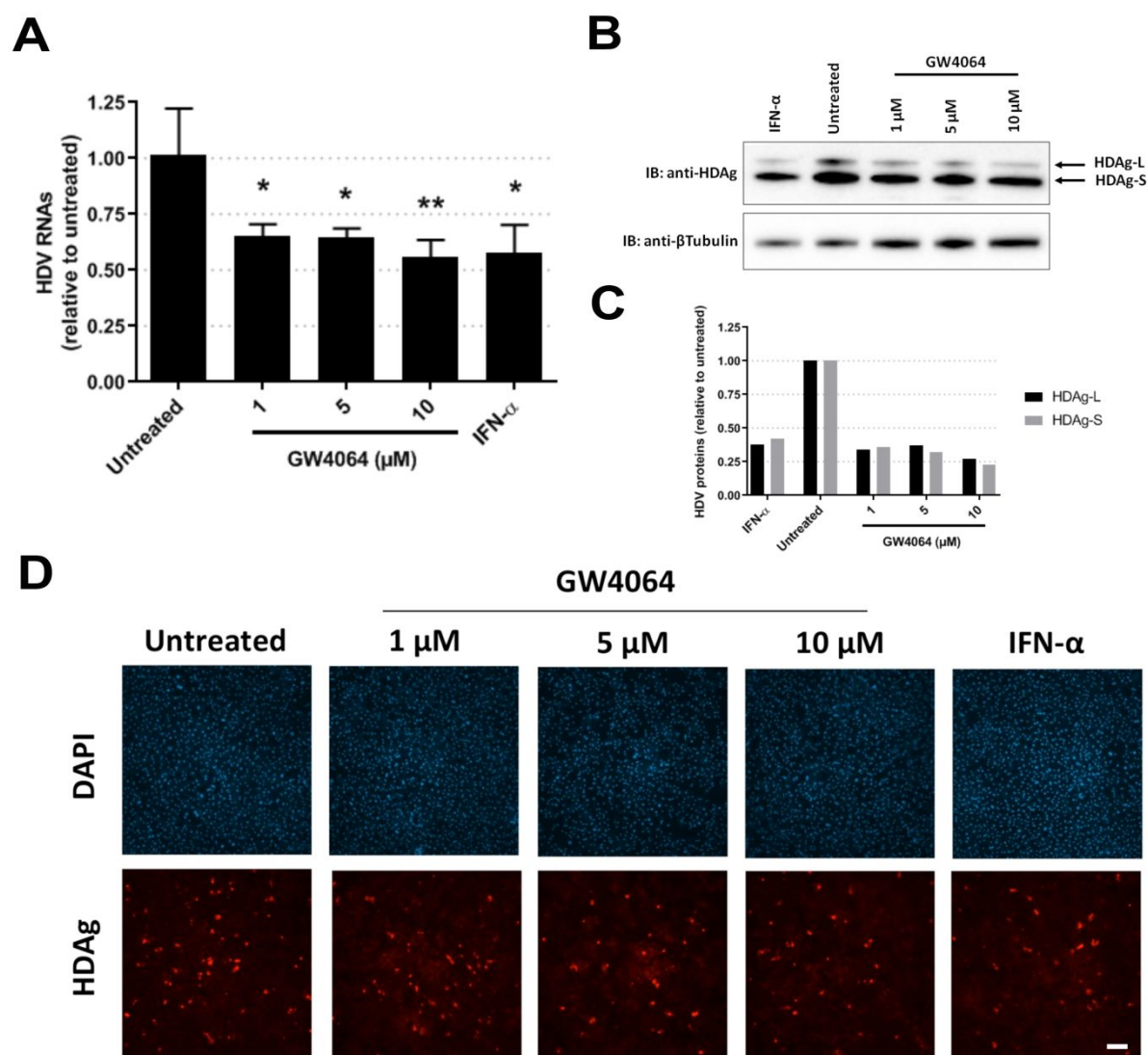


Figure S1. FXR ligand GW4064 decreases the levels of intracellular HDV RNAs and proteins in HBV-infected PHH superinfected with HDV. PHH were infected with HBV at a MOI of 100 vge per cell and 4 days later with HDV at a MOI of 10 vge per cell. 3 days post-HDV infection, cells were treated with 1, 5 or 10 μ M of GW4064, IFN- α (1000 IU/mL) or not. Cells were harvested 10 days post-treatment for cellular RNA and protein extraction or fixed with formaldehyde for immunofluorescence analyses. Intracellular HDV RNAs were quantified (A). Results are the mean \pm SD of one experiment performed with three biological replicates. Student's t-test, * p < 0.05, ** p < 0.01, *** p < 0.001. Analysis of the levels of HDV proteins by western blot analyses were performed using anti-HDV antibodies and anti- β -tubulin antibodies as a loading control (B). Densitometry analyses are presented as ratios of HDV proteins normalized to the levels of β -tubulin (C). Immunofluorescence analyses were performed using anti-HDV antibodies and nuclei DAPI staining (D). Scale bar: 200 μ m.

Figure S2

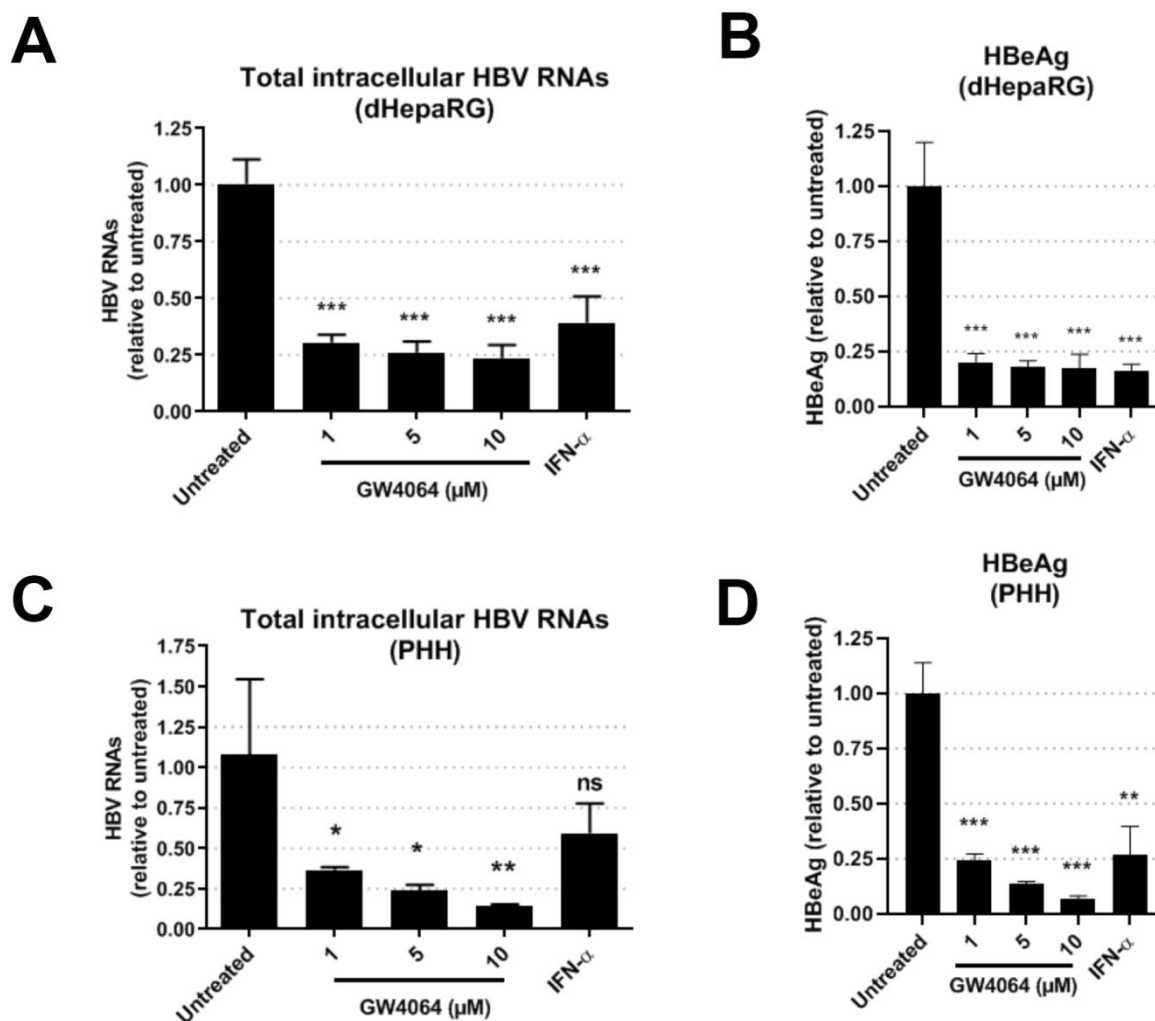


Figure S2. FXR ligand GW4064 decreases the levels of HBV replication markers in HBV-infected dHepaRG and PHH superinfected with HDV. dHepaRG cells or PHH were infected and treated as described for Fig. 1 and S1. Cells and supernatants were harvested 10 days post-treatment for quantification of intracellular HBV RNAs (A: dHepaRG cells ; C: PHH) and secreted HBe antigens (B: dHepaRG cells ; D: PHH). Results are the mean +/- SD of three experiments (dHepaRG) and one experiment (PHH) each performed with three biological replicates. Student's t-test *p < 0.05, **p < 0.01, ***p < 0.001, ns: not significant.

Figure S3

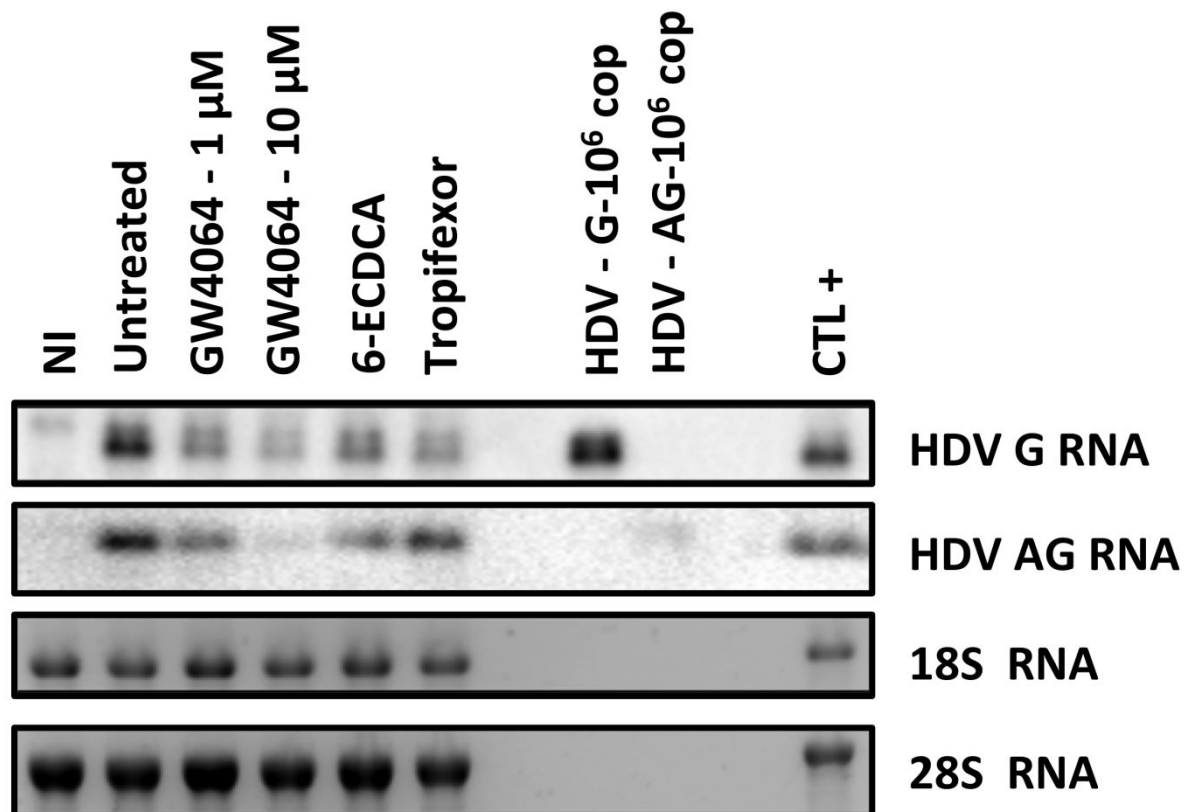


Figure S3. FXR ligands decrease the levels of genomic and antigenomic HDV RNAs in HDV-monoinfected dHepaRG cells. dHepaRG cells were infected with HDV at a MOI of 25 vge per cell. From day 4 to day 11 post-infection, cells were treated with 10 μ M of GW4064, 10 μ M of 6-ECDC and 1 μ M of tropifexor. Cells were harvested at day 11 post HDV infection and total RNAs were extracted. HDV genomic and antigenomic RNAs were analyzed by Northern Blot. NI: non infected; G RNA: genomic RNA; AG RNA: antigenomic RNA.

Figure S4

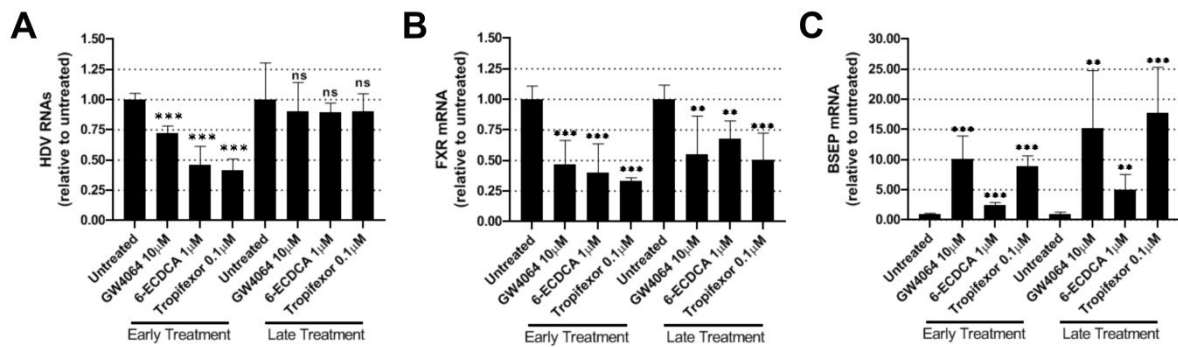


Figure S4. FXR ligands inhibit early phases of HDV infection in HDV-monoinfected PHH. PHH were infected with HDV at a MOI of 10 vge per cell. Cells were treated with 10 μM of GW4064, 1 μM of 6-ECDCA or 0.1 μM of trophifexor, either 1 day post-infection (early treatment) or 5 days post-infection (late treatment). Cells were harvested 10 days post-treatment. Total cellular RNAs were extracted and intracellular HDV RNAs (A), FXR mRNA (B) and BSEP mRNA (C) were quantified by RT-qPCR. Results are the mean \pm SD of two experiments each performed with 3 biological replicates. Data are normalized to untreated conditions for early and late treatments. Student's t-test, * $p < 0.05$, ** $p < 0.01$, *** $p < 0.001$, ns: not significant.

Figure S5

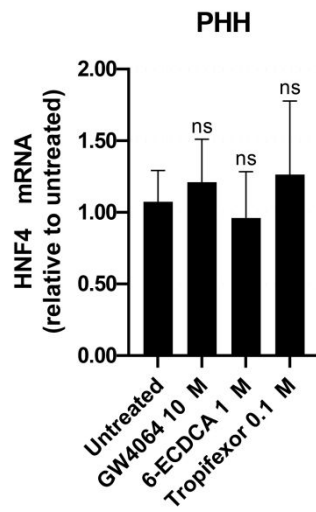


Figure S5. FXR ligands do not modify HNF4A mRNA expression in PHH. PHH were treated for 10 days with GW4064 at 10 μ M, 6-ECDCA at 1 μ M and tropifexor at 0.1 μ M. Total cellular RNAs were extracted and the level of HNF4A mRNA was quantified by RT-qPCR. Results are the mean \pm SD of three independent experiments each performed with three biological replicates. Student's t-test, ns: not significant.

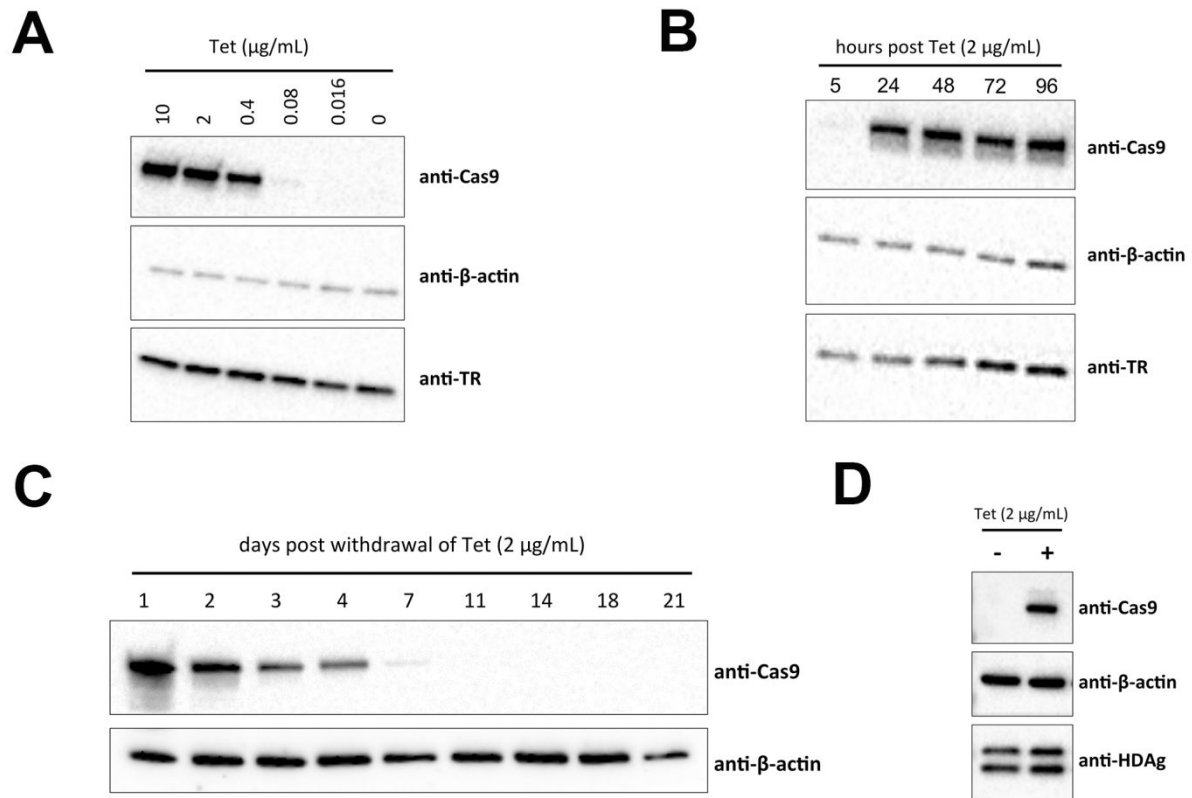
Figure S6

Figure S6. Characterization of HepaRG-TR-Cas9 cells. (A) dHepaRG-TR-Cas9 cells were treated with the indicated concentrations of Tetracyclin (Tet) for 3 days. (B) dHepaRG-TR-Cas9 cells were treated with Tet and collected at the indicated time. (C) dHepaRG-TR-Cas9 cells were treated with Tet for 24h and cells were collected at the indicated time after withdrawal of Tet. (D) dHepaRG-TR-Cas9 cells were treated or not with Tet for 1 day before infection with HDV at 100 vge/cell. Cells were collected at day 6 post-infection. (A, B, C, D) Western blot analyses were performed using the indicated antibodies.

Figure S7

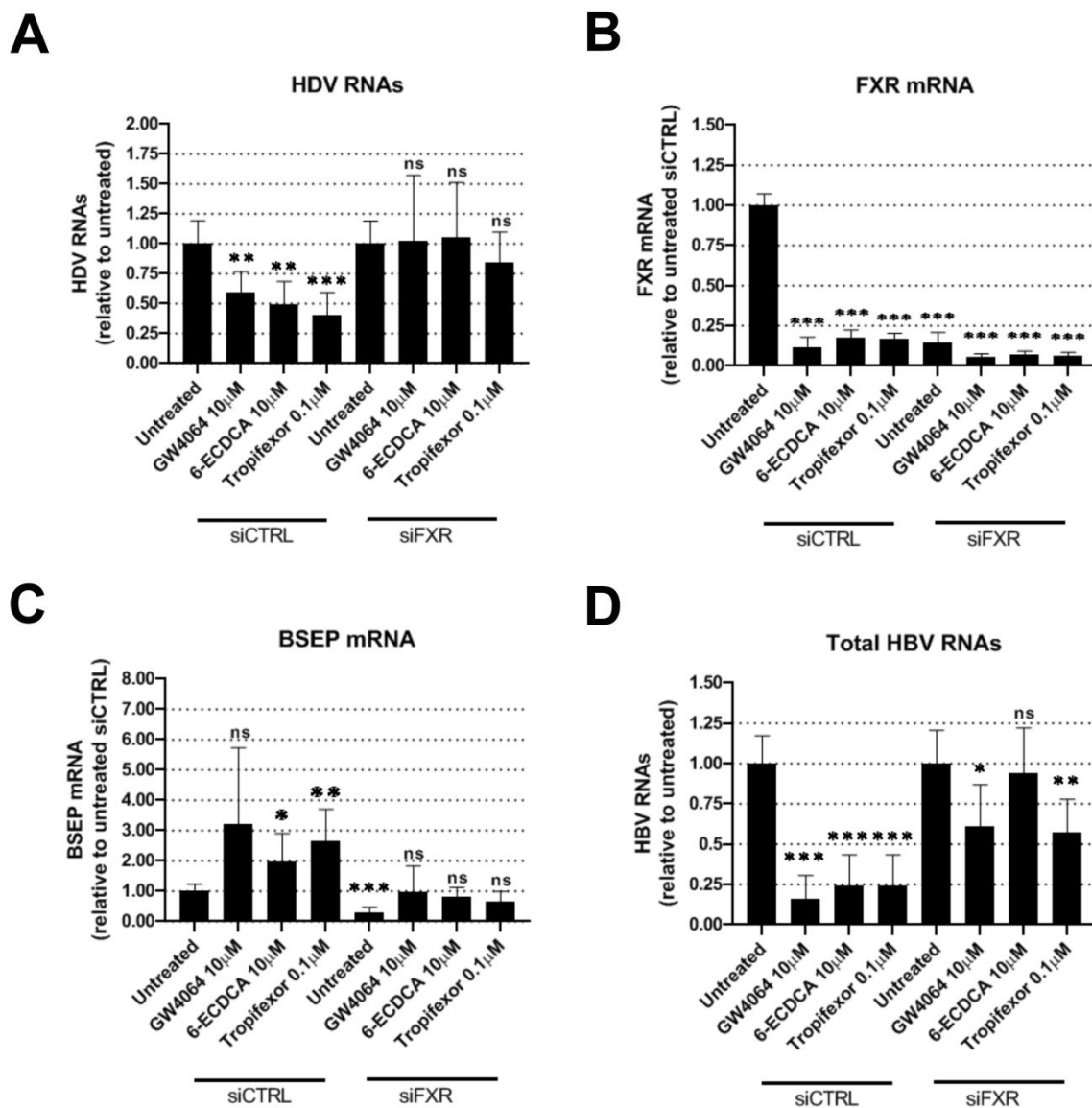


Figure S7. FXR silencing by siRNA abolishes the antiviral effect of FXR ligands on intracellular HDV RNAs in dHepaRG cells. dHepaRG cells were coinfecting with HBV at a MOI of 100 vge per cell and with HDV at a MOI of 10 vge per cell. 1 day post-infection, cells were transfected with a non-targeting siRNA control (siCTRL) or siRNA targeting FXR expression (siFXR). Following siRNA transfection, cells were treated or not for 7 days with GW4064, 6-ECDC or tropifexor. Cells were collected and intracellular RNAs were extracted. The levels of HDV RNAs (A), FXR mRNA (B), BSEP mRNA (C) and total HBV RNAs (D) were assessed by RT-qPCR analyses. Results are the mean \pm SD of two experiments each performed with 3 biological replicates. Data are normalized to untreated cells transfected with siCTRL. Student's t-test, * $p < 0.05$, ** $p < 0.01$, *** $p < 0.001$, ns: not significant.

Figure S8

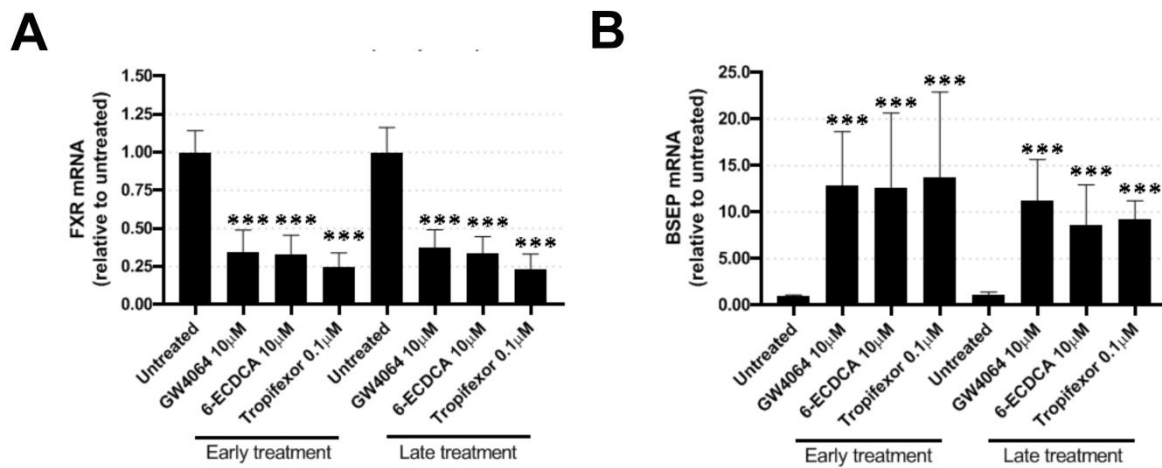


Figure S8. FXR ligands decrease FXR mRNA expression and induce BSEP mRNA expression in HBV/HDV coinfected dHepaRG cells. dHepaRG cells were monoinfected with HDV at a MOI of 10 vge per cell or coinfecting with HBV and HDV at a MOI of 100 and 10 vge per cell, respectively. Cells were treated with 10 μ M of GW4064 or 6-ECDC or 0.1 μ M of tropifexor, on day 1 post-infection for early treatment and on day 5 post-infection for late treatment. Cells were harvested 10 days post-treatment. Total cellular RNAs were extracted and FXR mRNA (A) and BSEP mRNA (B) were quantified by RT-qPCR. (C) Results are the mean \pm SD of three experiments each performed with 3 biological replicates. Data are normalized to the untreated conditions for early and late treatments. Student's t-test, *** p <0.001.

Figure S9.

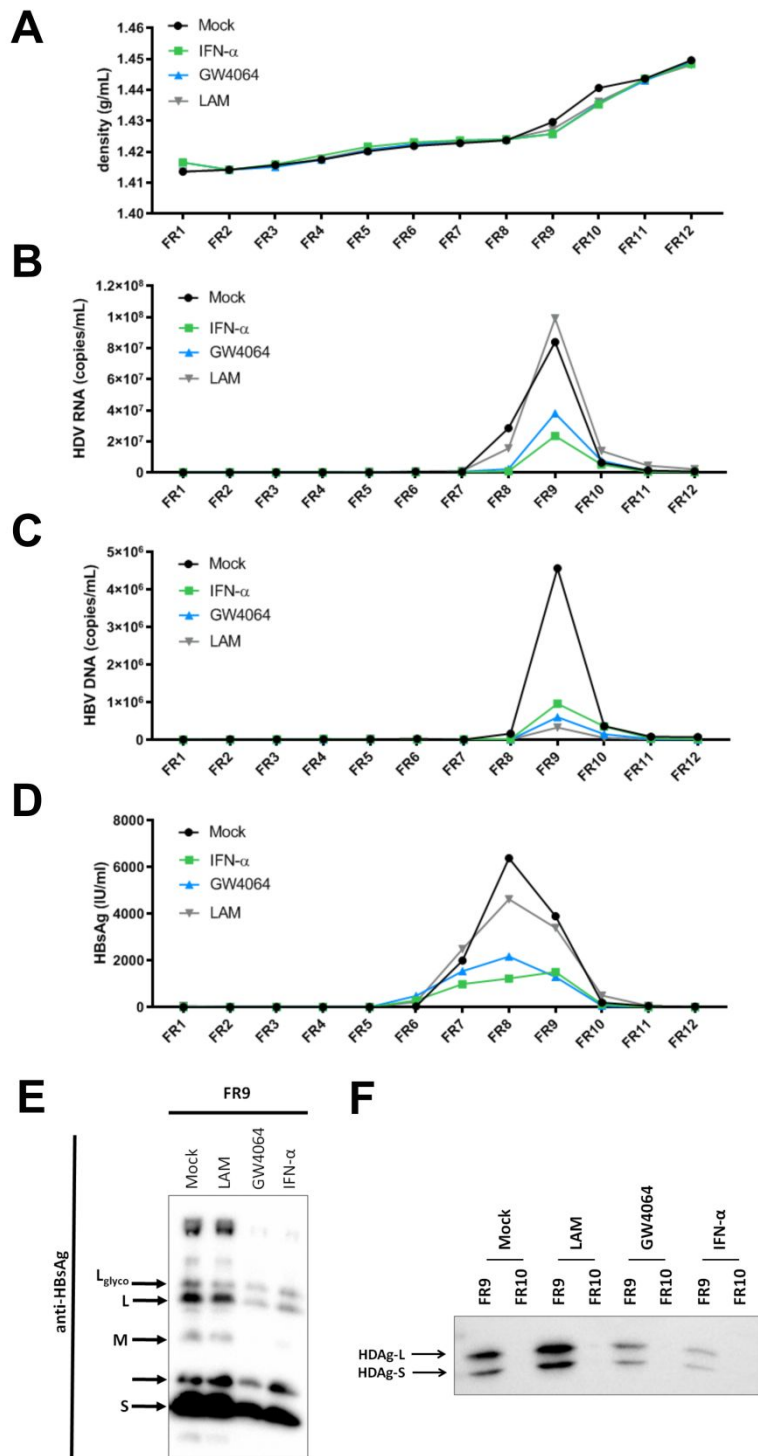


Figure S9. FXR ligand GW4064 does not modify buoyant density of secreted HDV particles.

dHepaRG cells were coinfecting with HBV and HDV with 500 vge/cell for HBV and 50 vge/cell for HDV. Cells were treated or not 3 days later with GW4064 (10 μ M), IFN- α (500 IU/mL) or LAM (10 μ M) for 10 days. Supernatants were collected at day 13 post-infection. Supernatants were collected, concentrated by PEG precipitation and submitted to iodixanol gradients overnight. Fractions (FR)

were collected and the density (A), the levels of HDV RNAs (B), HBV DNA (C) and HBsAg (D) were analysed by RT-qPCR, qPCR and ELISA. (E, F) WB analyses were performed in selected fractions using anti-HBsAg (E) and anti-HDAg (F) antibodies. LAM: lamivudine.

For Peer Review

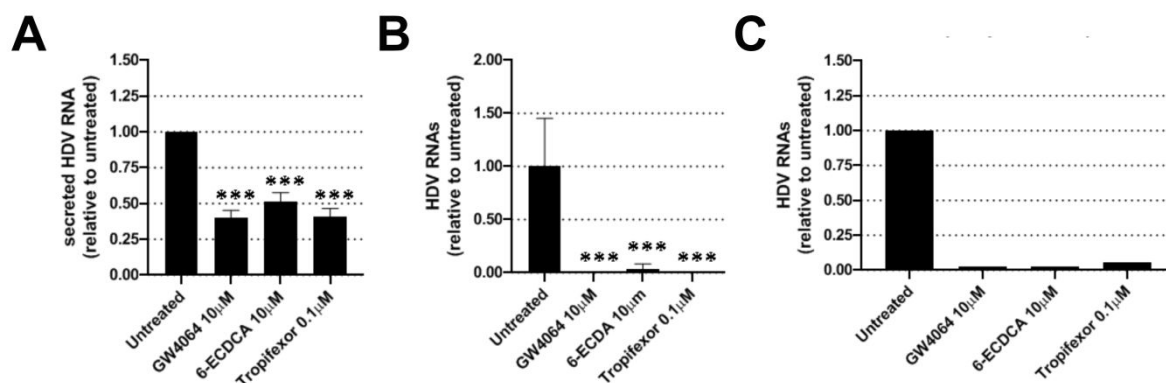
Figure S10.

Figure S10. FXR ligands decrease the infectivity of HDV particles. (A-B) dHepaRG were coinfecting with HBV and HDV at 100 vge and 10 vge per cell, respectively. Cells were treated at day 3 post-infection with GW4064 (10 μ M), 6-ECDCA (10 μ M) or tropifexor (0.1 μ M). 13 days post-infection, supernatants were collected and concentrated by PEG-precipitation. (A) The level of extracellular HDV RNAs were analyzed by qRT-PCR analyses. (B) Naïve HuH7.5-NTCP cells were infected with the different concentrated supernatants from treated dHepaRG cells with 500 vge per cell. Six days later, the levels of intracellular HDV RNAs were analysed by RT-qPCR. Results of RT-qPCR are the mean \pm SD of three independent experiments each performed with three biological replicates. Student's t-test *** p < 0.001. (C) Naïve dHepaRG cells were infected with PEG-precipitated HDV viruses collected from supernatants of dHepaRG cells following a 10-day treatment with the indicated FXR ligands. Six days later, the levels of intracellular HDV RNAs were analyzed by RT-qPCR. Results of RT-qPCR are the mean of one experiment performed with three biological replicates.